studied was Co, some relevant and interesting observations were made. (In the study, methylene and alkylidene fragments were treated as being similar.) They found that, in contrast to a methylene group coupling with a methyl group (alkyl mechanism growth step), the coupling of two methylene groups (alkylidene mechanism growth step) is exothermic and that no energy barrier exists along the reaction path. We believe the resulting chemisorbed ethylene is or becomes the growing chain in the alkylidene mechanism. We postulated that 2 in Scheme E represents this species, but its exact geometry may be different. It is interesting that Hoffmann et al. found that growth of an alkyl chain has an energy barrier and is endothermic.[26] Since we claim that all an alkyl chain undergoes is reductive elimination and β-elimination, it would be useful to calculate if those two elimination steps are indeed much faster than the potential growth step. Since the extended Hückel method is approximate and can be misleading when dealing with the energetics of bond formation, it would be helpful if more rigorous theoretical treatments of these species were available.

Conclusions

C_1+ SFA product distributions that contain both alkenes and alkanes and are produced from Fe FT catalysts are strong evidence against mechanisms that involve metal-bound alkyl or vinylidene groups as the growing chains. In order to avoid artificially constrained and possibly contradictory rate constants in the reaction mechanism, the chain growth step should be separated from the product formation step. We give both a general mechanism (Scheme D) and a specific example (alkylidene mechanism, Schemes E–G) describing how this separation of chain growth and product formation can be accomplished. The alkylidene mechanism can account for observed C_1+ SFA product distributions containing mixtures of alkenes and alkanes, methyl- and ethyl-branched hydrocarbons, and no quaternary carbons in a straightforward way. The alkylidene mechanism is also consistent with spectroscopic data and results from a theoretical study of FT catalysts. If this mechanism is correct, the way to reduce the methane yield relative to the C_2+ alkene yield in a FT reaction is to make the dehydrogenation rate of the methyl group to a methylene group competitive with the reductive-elimination rate of the methyl group to methane. Also, consideration of this mechanism may be useful when experiments are designed to elucidate the FT mechanism.

Acknowledgment. We gratefully acknowledge T. R. Hughes for his helpful discussions.

Registry No. CO, 630-08-0; Fe, 7439-89-6.

Correlation of Pour Point of Gas Oil and Vacuum Gas Oil Fractions with Compositional Parameters

R. Krishna,* G. C. Joshi, R. C. Purohit, K. M. Agrawal, P. S. Verma, and S. Bhattacharjee

Indian Institute of Petroleum, Dehra Dun 248 005, India

Received April 28, 1988. Revised Manuscript Received September 6, 1988

We have carried out a detailed investigation of the pour points (PPt) of gas oil (GO) (250–375 °C boiling range) and vacuum gas oil (VGO) (375–500 °C) fractions obtained from Bombay High crude oil. The aim of the study was to obtain an insight into the dependence of the pour point on compositional parameters such as the *n*-paraffin concentration (PC) and the influence of the length of the *n*-paraffinic chain (CL). The experimental work consisted of (i) detailed characterization of both narrow 25 °C cuts along with the two broad cuts (250–375 and 375–500 °C) and (ii) a study of the effect of progressive addition of *n*-paraffin concentrates (urea-adductable portions) of the narrow cuts on the cold-flow behavior of the broad cuts from which the urea adductables have been removed. A simple correlation has been put forward that allows the prediction of the pour point from a knowledge of PC and CL. The study should provide a rational basis for a fundamental predictive method for the cold-flow behavior of GO and VGO fractions.

Introduction

Pour point and other cold-flow properties in the distillate fuels are primarily controlled by the *n*-paraffinic components present in the solvent matrix.[1-5] When the distillate fuels are cooled, "wax" crystals, containing predominantly *n*-paraffins of the high chain lengths, separate out. These crystals may interlock, forming a cagelike structure that entraps the solvent molecules, and at a certan stage the fuel ceases to flow. Even if 1 or 2% of separated crystals are thus formed, cessation of the free flow of the fuel may result;[3] the temperatue at which this occurs is the pour point.

While some attempts have been made to correlate one or more cold-flow properties with average molecular weight and *n*-paraffin content of the fuel,[4-7] there appears to be

* To whom correspondence is to be addressed.

(1) Turner, W. R. *Ind. Eng. Chem. Prod. Res. Dev.* **1971**, *10*, 238–260.
(2) Pass, F. J.; Csoklich, Ch.; Wastl, K. *Proc. 7th World Pet. Congr.* **1967**, *8*, 129–139.
(3) Rossemyr, L. I. *Ind. Eng. Prod. Res. Dev.* **1979**, *18*, 227–230.
(4) Knepper, J. I.; Hutton, R. P. *Hydrocarbon Process.* **1975**, *54*, 129–136.
(5) Hu, J.; Burns, A. M. *Hydrocarbon Process.* **1970**, *49*, 213–216.

0887-0624/89/2503-0015$01.50/0

no systematic study to quantify the effect of *n*-paraffin concentration and the chain length of the *n*-paraffin molecules. There is also a need for a better understanding of the role of solvent matrix in determining the cold-flow properties. In the present work we undertake a systematic experimental study to quantify the factors that affect the pour point of GO and VGO fractions derived from a particularly paraffinic crude: Bombay High crude oil. The detailed characterization of the two broad fractions, GO and VGO, and narrow 25 °C cuts of these fractions provides the basis of the correlations suggested in this paper.

Experimental Section

Preparation of Distillate Fractions. The crude oil, collected from the Bombay High offshore platform before injection of various additives, was distilled in a pilot distillation unit operating at atmospheric as well as reduced pressure. After removal of water and forerun up to 250 °C, the desired broad cut fractions (BC1, 250–375 °C; BC2, 375–500 °C) were collected at reduced pressure to avoid thermal decomposition. These broad cuts were further fractionated at reduced pressure to five narrow (25 °C) boiling range fractions. All 12 (10 + 2) of these fractions were characterized for pour point, cloud point (CPt), and cold filter plugging point (CFPP). Standard IP/ASTM procedures were followed for cold-flow tests.

Urea Adduction of Distillate Fractions. Each of the 12 fractions obtained above was subjected to urea adduction by using the procedure described below.

A solution of the sample to be adducted was prepared in dichloromethane (1 g of sample/3 mL of solvent). The solution was mixed with a saturated solution of urea in methanol (1:5 sample/urea weight ratio) in an Erlenmeyer flask. The contents were swirled at room temperature (24 ± 2 °C) and set aside for adduct formation. The adduct was recovered by filtration in a Büchner funnel under suction with the help of dichloromethane solvent, which was used for transfer of the adduct and washing of the filter cake. After drying, the adduct was decomposed by hot water and the urea adductables (containing predominantly *n*-paraffins) were recovered and weighed. The filtrate was treated for the recovery of nonadductable hydrocarbons. The drop melting points of the urea adductables were determined by using ASTM D-127.

Carbon Number Distribution of the *n*-Paraffins in the Urea-Adductable Portions of the Fractions. The carbon number distribution of the urea adductables was determined by gas chromatography. The method used was an adaptation of IP 372. A stainless-steel column (2 m × 3.2 mm) packed with 5% SE-30 on chromosorb W (80-100 mesh) was used with temperature programming and nitrogen as carrier gas. The intensity of signals from *n*-paraffin as well as the envelope from nonnormal paraffins at the base of the *n*-paraffin peaks were measured for the carbon numbers of the corresponding *n*-paraffin peak. A typical chromatogram is shown in Figure 1.

To quantify the effect of *n*-paraffin concentration in controlling pour point and also to ascertain its dependence on the environment matrix, two further data sets were generated in the following manner.

Urea adductables obtained from the 375–500 °C broad and narrow fractions were added in progressively increasing concentration to the 375–500 °C denormalized base from which the urea adductables have been removed, and the resulting pour points were recorded. Similarly, urea adductables obtained from the 250–425 °C narrow cuts were added into the denormalized 250–375 °C base, and the resultant pour points were recorded; see Table II. For each urea-adductable fraction added, the carbon number distribution was determined, from which the concentration of *n*-paraffins (of chain length larger than 15) could be determined.

Table I summarizes the cold-flow and other physical properties for the broad and narrow cuts. It can be seen that the nonnormal paraffin content in the urea adductables ranges from 6 to 11%.

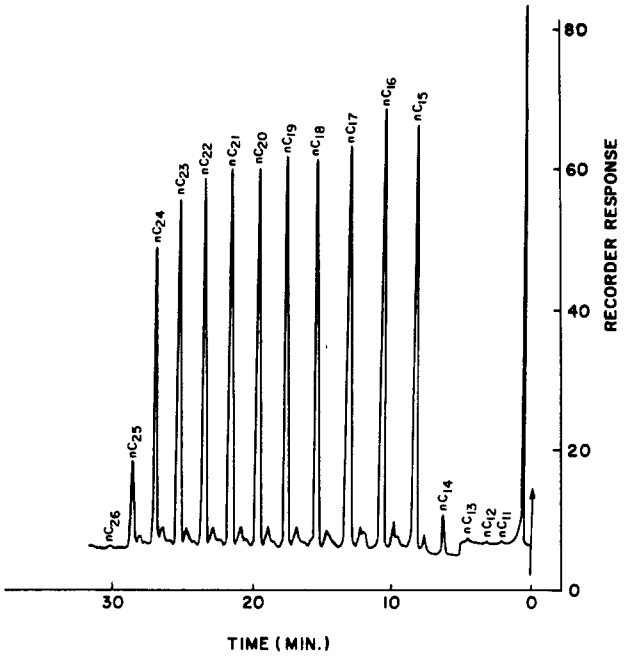

Figure 1. Gas chromatogram of urea-adductable-separated 250–375 °C fraction.

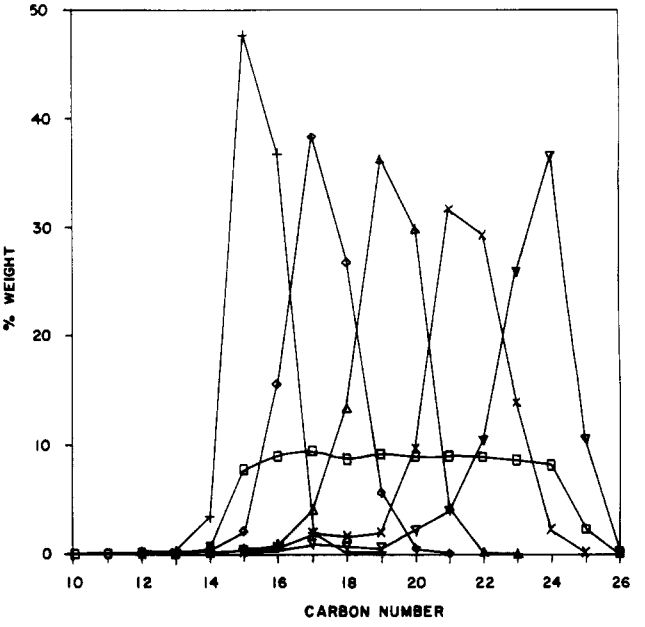

Figure 2. Carbon number distribution of *n*-paraffins present in the broad and narrow cuts in the 250–375 °C boiling range: BC1 (□); NC1 (+); NC2 (◇); NC3 (△); NC4 (×); NC5 (▽).

Results and Discussion

The carbon number distribution of the *n*-paraffins present in the 250–375 °C broad and narrow fractions have been plotted in Figure 2, and those for the 375–500 °C fractions have been plotted in Figure 3. It is observed that the distribution is nearly Gaussian. It is observed that the carbon number distribution of the two broad cuts BC1 and BC2 is the envelope of the distributions of their respective narrow fractions, weighted according to their respective yields.

From the carbon number distribution, the average chain length of the *n*-paraffins (CL) can be calculated, and the values for the various fractions are given in Table I. It is to be expected that the pour point of any cut will not be affected by the *n*-paraffin molecules shorter than 15 in carbon chain length.[8] With this in mind, concentration

(6) Riazi, M. R.; Daubert, T. E. *Hydrocarbon Process.* **1987**, *66*, 81–83.
(7) Tsang, C. Y.; Ker, V. S. F.; Miranda, R. D.; Wesch, J. C. *Oil Gas J.* **1988** (March 28), 33–38.

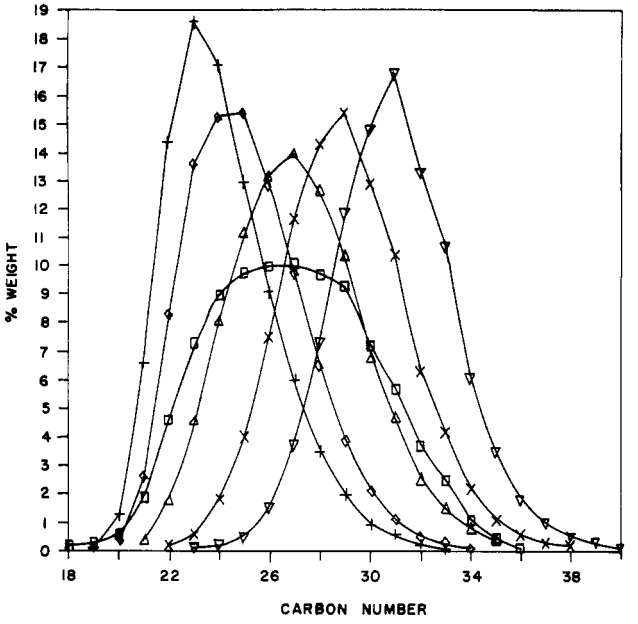

Figure 3. Carbon number distribution of *n*-paraffins present in the broad and narrow cuts in the 375–500 °C boiling range: BC2 (□); NC6 (+); NC7 (◇); NC8 (△); NC9 (×); NC10 (▽).

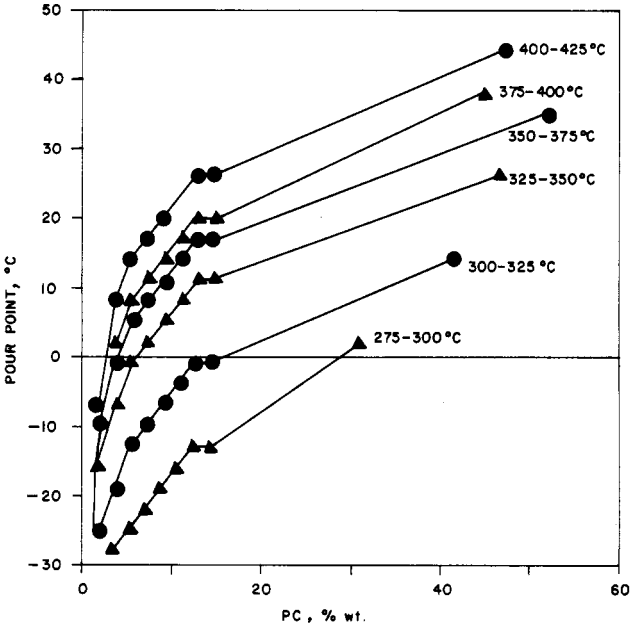

Figure 4. Effect of *n*-paraffin concentration on the pour points of the denormalized 250–375 °C base.

of *n*-paraffins in weight percent having a chain length longer than 15 have been shown in Table I; these have been denoted as PC. We have also listed in Table I the melting point of the *n*-paraffin molecule with the average carbon number of the fraction under consideration, calculated from the expression[9]

$$\text{mp} = [415M/(M + 95)] - 273 \quad (1)$$

where M is the molecular weight defined by

$$M = 14n + 2 \quad (2)$$

n being the carbon number of the *n*-paraffin molecule; for mixtures of *n*-paraffins, n may be identified with the average chain length. The drop melting points of the urea adductables as reported in Table I are seen to be 3–7 °C lower than the values of mp calculated according to eq 1 and 2, using the average chain length of the normal paraffins. The difference may be attributed to the effect of the small amounts of nonnormal paraffins in the urea adductables, which will have the (expected) effect of lowering the melting point.

(8) Reddy, S. R.; McMillan, M. L. *SAE Trans.* 1981, Paper 811181.
(9) Freund, M.; Csikos, R.; Keszthelyi, S.; Mozes, G. *Paraffin Products, Properties, Technologies, Applications*; Mozes, G., Ed.; Developments in Petroleum Science 14, Elsevier: Amsterdam, 1982; p 26.

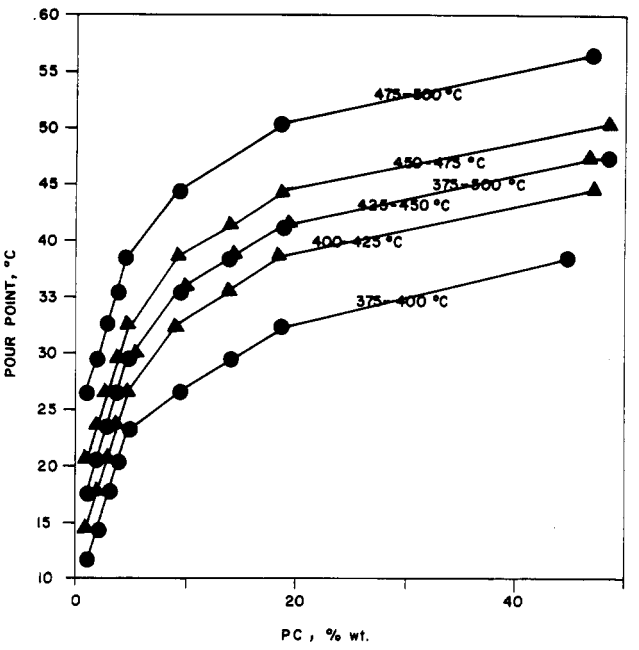

Figure 5. Effect of *n*-paraffin concentration on the pour points of the denormalized 375–500 °C base.

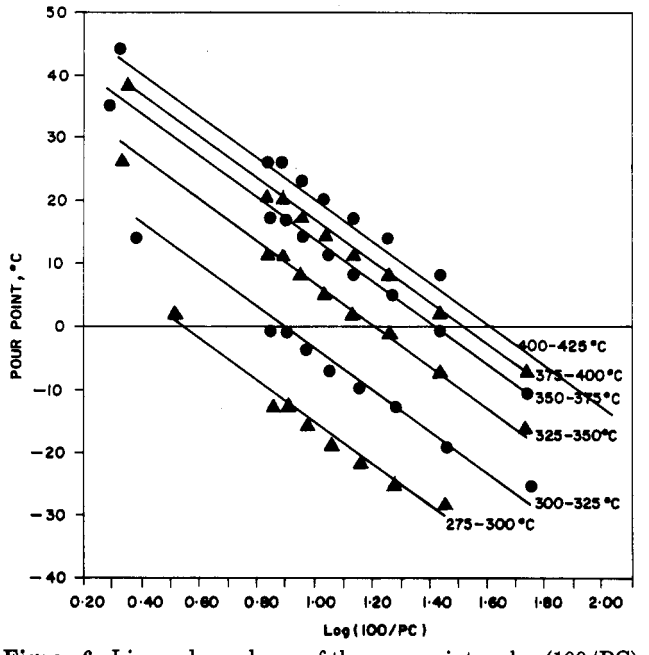

Figure 6. Linear dependence of the pour point on log (100/PC) obtained for the data set of Figure 4.

Effect of *n*-Paraffin Concentration and Chain Length on Pour Point. The effect of progressive addition of *n*-paraffin concentrate (urea adductable portions) on pour point was similar for both 250–375 °C and 375–500 °C bases. The pour point varies with the *n*-paraffin concentration, PC, in a nonlinear manner; for any fraction the pour point initially increases sharply with an increase in paraffin concentration, PC, and thereafter the rate of increase decreases. Figures 4 and5 show these *n*-paraffin

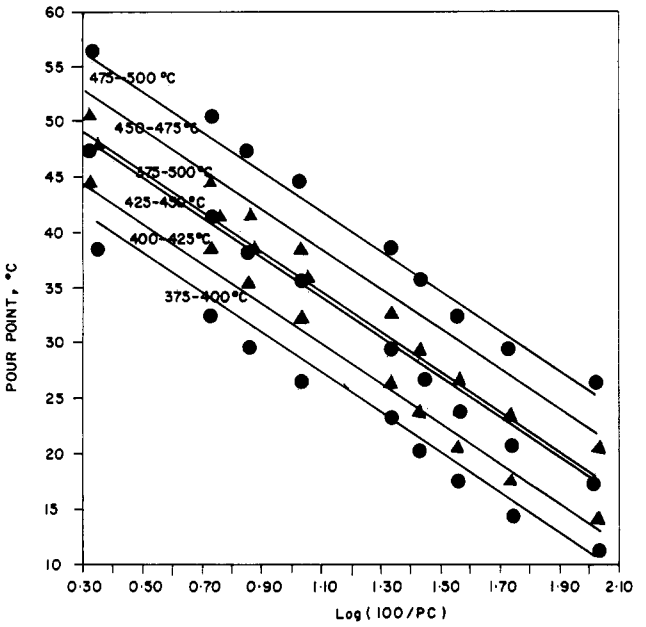

Figure 7. Linear dependence of the pour point on log (100/PC) obtained for the data set of Figure 5.

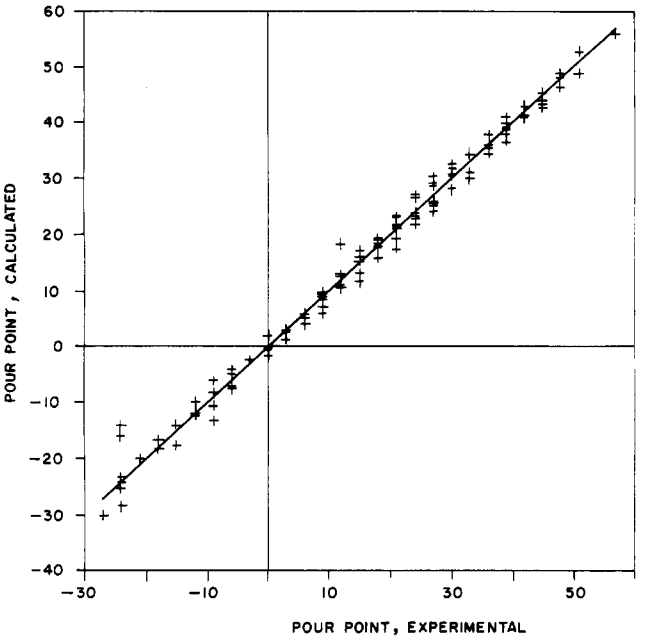

Figure 8. Comparison of experimentally determined pour points and those determined from eq 5–7.

concentration dependences for the 250–375 °C and 375–500 °C fractions respectively. Quantifying this nonlinear dependence, from Figures 6 and 7, it is observed that the pour point of each narrow cut varies linearly with log (100/PC). It is further observed that the straight lines obtained in Figures 6 and 7 are parallel, signifying that the dependence of the pour point on PC is independent of the chain length for the particular denormalized base under consideration. We may describe straight line relationships of Figures 6 and 7 by

$$PPt = A0 \log (100/PC) + B1 \quad (3)$$

where the "intercept" B1 depends on the particular fraction under consideration, or in other words B1 depends on CL. The intercept B1 can be interpreted as the pour point of the fraction when the paraffin concentration PC equals 100%. At 100% paraffin concentration we should expect that the value of B1 should be related to the melting point of the fraction. From eq 1 it can be seen that the melting point varies approximately as the inverse of the CL (i.e. the value of n). Therefore we might expect a linear relationship between B1 and 1/CL, i.e.

$$B1 = A1(1/CL) + A2 \quad (4)$$

Combining eq 3 and 4, we obtain the correlation for the pour point as follows

$$PPt = A0 \log (100/PC) + A1(1/CL) + A2 \quad (5)$$

From a regression analysis of the two data sets (250–375 and 375–500 °C denormalized bases), the coefficients A0, A1 and A2 can be determined; the results of this analysis are as follows: for the 250–375 °C denormalized base

$$A0 = -33.33;\ A1 = -1923.4;\ A2 = 130.1 \quad (6)$$

with a standard error in the pour point estimate of 2.45 °C; for the 375–500 °C denormalized base

$$A0 = -18.09;\ A1 = -1591.5;\ A2 = 113.2 \quad (7)$$

with a standard error in the pour point estimate of 1.62 °C. A comparison of the measured and estimated pour points for the total data set, using the correlations given by eq 5–7, are shown in Figure 8. The overall standard error in the estimate of the pour point for the range

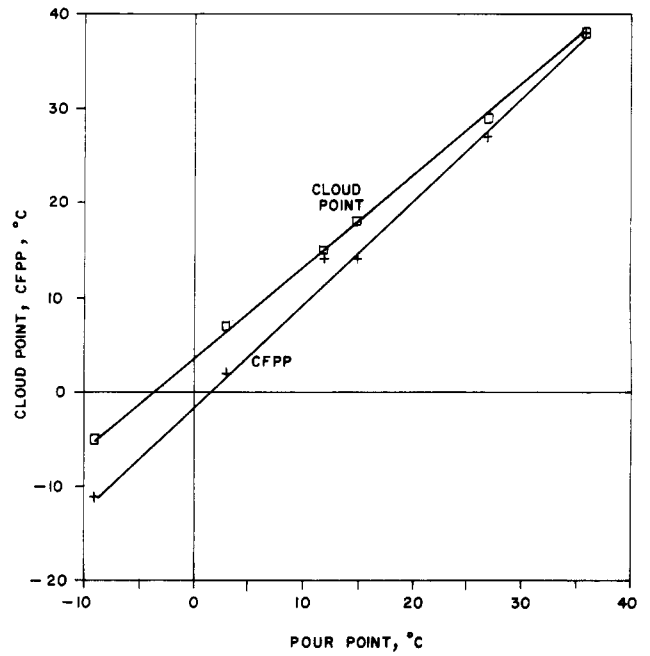

Figure 9. Linear interrelationship between the pour point and the cloud point and CFPP.

250–500 °C is 2.06 °C, which is well within the repeatability of the measurement of the pour point (±3 °C).

Since pour point shows a good correlation with the cloud point (CPt) and the cold filter plugging point (CFPP) (cf. Figure 9), it is expected that CPt and CFPP may be correlated in the same manner as described by eq 5.

Conclusions

From a detailed characterization of 2 broad cuts (250–375 °C and 375–500 °C) and 10 narrow cuts obtained from Bombay High crude oil, the dependence of pour point with n-paraffin concentration (PC) and average n-paraffinic chain length (CL) has been quantitatively established in terms of eq 5. Though the study has been restricted to Bombay High crude oil fractions, it is to be expected that relationships given by eq 5 would hold for other crudes as well, with a different set of coefficients A0,

Table I. Physicochemical Properties of 250–375 and 375–500 °C Fractions of Bombay High Crude Oil

	fractions											
properties	250–375 °C BC1	250–275 °C NC1	275–300 °C NC2	300–325 °C NC3	325–350 °C NC4	350–375 °C NC5	375–500 °C- BC2	375–400 °C NC6	400–425 °C NC7	425–450 °C NC8	450–475 °C NC9	475–500 °C NC10
yield on crude oil, wt %	24.97	5.07	6.34	4.85	4.79	3.92	25.3	5.5	5.7	5.4	5.1	3.6
pour point, °C	12	–9	3	15	27	36	48	39	45	48	51	57
cloud point, °C	15	–5	7	18	29	38						
CFPP, °C	14	–11	2	14	27	38						
kinematic viscosity (at 70 °C), cSt	2.49	1.73	2.32	3.06	3.96	5.07	9.12	6.05	7.79	9.00	9.88	14.64
aniline point, °C	77.5	62.8	78.0	80.4	88.7	95.5	101.8	94.4	99.8	102.5	105.5	110.9
refractive index at 70 °C, deg	...	1.4560	1.4512	1.4582	1.4565	1.4591	1.4648	1.4635	1.4640	1.4642	1.4644	1.4651
density [$d(15/4)$], g/cm^3	0.8541	0.8548	0.8450	0.8597	0.8547	0.8605	0.8915	0.8715	0.8856	0.8881	0.8891	0.9063
% carbon	85.68	86.80	85.70	86.10	85.60	85.86	86.33					
% hydrogen	14.16	13.10	13.42	12.73	13.07	12.88	13.20					
mid boiling temp (T50), °C	...	262.5	287.5	312.5	337.5	362.5	...	387.5	412.5	437.5	462.5	487.5
n-paraffin concn (PC), wt %	38.45	27.64	30.79	41.41	46.7	52.13	46.8	44.88	47.28	48.41	48.72	47.05
average *n*-paraffinic chain length (CL)	19.6	15.4	17.2	19.2	21.4	23.2	26.89	24.13	25.12	27.14	29.05	31.0
mol wt	274	220	247	273	302	319	378	339	353	380	409	437
drop mp, °C	32.0	11.0	17.9	28.2	38.4	42.9	57.6	48.0	54.0	57.0	59.0	65.0
mp calcd from eq 1	35.85	15.88	25.29	34.22	42.59	48.53	58.73	51.33	54.13	59.34	63.73	67.75
% nonnormal paraffins in urea adductables	9.6	9.7	11.1	10.8	7.6	8.7	6.4	6.5	7.3	6.9	6.3	5.9

Table II. Effect of Successive Urea-Adductable Addition on Pour Points of the Denormalized Bases for 250–375 and 375–500 °C Fractions

	pour point for urea adductables added, °C													
	denormalized 250–375 °C base								denormalized 375–500 °C base					
% urea adductables added	250–375 °C BC1	250–275 °C NC1	275–300 °C NC2	300–325 °C NC3	325–350 °C NC4	350–375 °C NC5	375–400 °C NC6	400–425 °C NC7	375–500 °C BC2	375–400 °C NC6	400–425 °C NC7	425–450 °C NC8	450–475 °C NC9	475–500 °C NC10
0	<–27	<–27	<–27	<–27	<–27	<–27	<–27	<–27	12	12	12	12	12	12
1	<–27	<–27	<–27	<–27	<–27	<–27	<–27	–24	21	12	15	18	21	27
2	<–27	<–27	<–27	–24	–15	–9	–6	–6	24	15	18	21	24	30
3									27	18	21	24	27	33
4	–24	<–27	–27	–18	–6	0	3	9	30	21	24	27	30	36
5									33	24	27	30	33	39
6		<–27	–24	–12	0	6	9	15						
8	–9	<–27	–21	–9	3	9	12	18						
10		<–27	–18	–6	6	12	15	21	36	27	33	36	39	45
12	0	–27	–15	–3	9	15	18	24						
14		–24	–12	0	12	18	21	27						
15									39	30	36	39	42	48
16	6	–24	–12	0	12	18	21	27						
20	9								42	33	39	42	45	51
100[a]	32	11	17.9	28.2	38.4	42.9	48	54	57.6	48	54	57	59	65

[a] Values indicated represent drop melting point (°C) of urea adductables

A1, and A2. Further study is required to establish the dependence of the parameters A0, A1, and A2 on the detailed chemical compositions present in the fractions.

Glossary

A0, A1, A2	parameters defined by eq 5
BC1	250–375 °C broad cut
BC2	375–500 °C broad cut
CFPP	cold filter plugging point, °C
CL	average *n*-paraffinic chain length
CPt	cloud point, °C
GO	gas oil
NC1–NC10	narrow 25 °C cuts
PC	*n*-paraffin concentration, wt %
PPt	pour point, °C
T50	midboiling temperature, °C
VGO	vacuum gas oil

Registry No. Dodecane, 112-40-3; tridecane, 629-50-5; tetradecane, 629-59-4; pentadecane, 629-62-9; hexadecane, 544-76-3; heptadecane, 629-78-7; octadecane, 593-45-3; nonadecane, 629-92-5; eicosane, 112-95-8; heneicosane, 629-94-7; docosane, 629-97-0; tricosane, 638-67-5; tetracosane, 646-31-1; pentacosane, 629-99-2; hexacosane, 630-01-3; heptacosane, 593-49-7; octacosane, 630-02-4; triacontane, 638-68-6; hentriacontane, 630-04-6; dotriacontane, 544-85-4; tritriacontane, 630-05-7; tetratriacontane, 14167-59-0; pentatriacontane, 630-07-9; hextriacontane, 630-06-8; heptatriacontane, 7194-84-5; octatriacontane, 7194-85-6; nonatriacontane, 7194-86-7; nonacosane, 630-03-5.

Assessing Distillate Fuel Storage Stability by Oxygen Overpressure

Dennis R. Hardy,*,† Robert N. Hazlett,† Erna J. Beal,† and Jack C. Burnett‡

Navy Technology Center For Safety and Survivability, Code 6180, Naval Research Laboratory, Washington, D.C. 20375-5000, and GEO-Centers, Inc., Fort Washington, Maryland 20744

Received August 5, 1988. Revised Manuscript Received October 20, 1988

This paper describes a new method for predicting distillate fuel's tendency for forming deleterious fuel insolubles during ambient storage. Oxygen is forced into solution in the fuel at pressures up to 794 kPa (100 psig). The fuel is stressed under conditions of accelerated storage. The method then makes use of gravimetric determination of the total insolubles formed. This rapid and precise method is predictive for up to 3 years of ambient conditions. It has been used to rank additive-free fuels over a wide range of storage stabilities and has also been useful in assessing the relative effectiveness of middle-distillate fuel stabilizer (antioxidant) additives.

Introduction

Currently utilized methods for assessing storage stability of middle-distillate fuels suffer a variety of drawbacks. Lower temperature bottle tests are generally the best indicators of storage stability of a particular fuel, but meaningful results require storage at 40–50 °C for between 12 and 18 weeks. At temperatures of 80 °C and above, bottle storage tests can usually be completed in a reasonably short time, as little as 24 h, but these tests are generally poor indicators of actual ambient fuel reactions leading to insoluble products.[1,2]

One test widely used in both the commercial and military sectors as a rapid assessment of fuel storage oxidative stability is the ASTM D 2274 method.[3] This test has several major problems. It is not a good predictor of storage stability for freshly refined middle-distillate fuels that contain any catalytically cracked stocks. Another problem is the fact that the recommended fuel incubation time of 16 h is too short for many fuels.[1,2] This leads to two further related problems. The total amount of insolubles formed is very low and quite difficult to quantify. Second, and more important, it allows a potentially unstable fuel to pass the test. Recent attempts to circumvent this second problem in the military have been to lower the pass criterion (rather than increase the incubation test time). In the past 6 years the military procurement specification maximum has been lowered from 2.5 to 1.5 mg/100 mL of fuel. The primary effect of this has been to worsen the precision of replicate analyses both within the laboratories and between laboratories.

The present method evolved from attempts to measure oxygen uptake in middle-distillate fuels using an ASTM D 525 oxidation bomb apparatus at elevated pressures of pure oxygen. During these experiments, it was apparent that the actual chemically involved oxygen uptake leading to insoluble production was too small to measure by this technique and further work in this area was abandoned. Other very interesting effects were noted however. Oxygen solubilization in the fuel occurred very slowly, large amounts of insolubles formed in short times, and good precision was obtained for replicates when the insolubles were gravimetrically determined. This led to the development of a procedure to purposely accelerate the reactions leading to the formation of fuel insoluble sediments

† Naval Research Laboratory.
‡ GEO-Centers, Inc.

(1) Stirling, K. Q.; Brinkman, D. W. *NIPER-352*; National Institute for Petroleum and Energy Research: Bartlesville, OK, 1988.
(2) Hardy, D. R.; Beal, E. J.; Hazlett, R. N.; Burnett, J. C. Evaluation of Commercial Stability Additives For Naval Distillate Fuel. In *Proceedings of the Third International Conference on Stability and Handling of Liquid Fuels*; Institute of Petroleum: London; in press.
(3) *Oxidation Stability of Distillate Fuel Oil*; ASTM D 2274-74; American Society for Testing and Materials: Philadelphia, PA, 1982.

0887-0624/89/2503-0020$01.50/0